Cut & chip wear of rubbers in a range from low up to high severity conditions

R. Stoček [a,b,*], G. Heinrich [c], R. Kipscholl [a,d], O. Kratina [b]

[a] Polymer Research Lab s.r.o., Nad Ovčírnou 3685, 76001 Zlín, Czechia
[b] Centre of Polymer Systems, Tomas Bata University in Zlín, tř. Tomáše Bati 5678, 76001 Zlín, Czechia
[c] Technische Universität Dresden, Institut für Textilmaschinen und Textile Hochleistungswerkstofftechnik, Hohe Str. 6, 01069 Dresden, Germany
[d] Coesfeld GmbH & Co. KG, Tronjestraße 8, 44319 Dortmund, Germany

ARTICLE INFO

ABSTRACT

The development of cut and chip (CC) resistant rubber articles, composed of rubber blends, requires a detailed understanding and a controlled estimation of the CC behavior of each separate rubber component within the blend in a wide range of severity conditions. This study is focused on comparative CC investigations of NR, SBR and NR/SBR (50:50) rubber blends using an Instrumented Chip and Cut Analyser (ICCA, Coesfeld GmbH, Germany) in a broad range of loading conditions. We show the results for the CC effects dependant on the applied normal forces from 90 to 200 N during cyclic impact damaging and the evolution of the temperature on the surface of the damaged specimen. We find significant differences between the used rubbers regarding dependence on the damage parameters and temperature on the normal load which determines the severity to which the rubber is exposed. In the case of NR evolving the CC damage and temperature goes through a maximum at critical values of the impacting normal load. This effect is briefly discussed in the context of the appearance of strain-induced crystallization (SIC) in the NR during cyclic impacts above a critical level. The results impressively explain the empirical preference for NR or NR-blends in practice when it comes to minimizing CC wear.

Introduction

When operating rubber products, such as tires, conveyor belts, rubber tracks, these are exposed to harsh severity conditions and one observes Cut & Chip (CC) wear phenomena as shown in Fig. 1. Sometimes, these wear phenomena are also termed as CCC which stands for cut, chip and chunk wear field conditions [1]. In the case of tires, CC wear refers to the detachment or breakage of rubber material from their treads when riding on a rough road surface (e.g., gravel roads, roots, stalks). This is most commonly associated with off-the-road tires (OTR), light truck (LTT) and SUV tires, however the phenomenon is also observed with highway truck tires as well as all-season passenger car tires. In the case of conveyor belts, CC arises when transporting gravel or any other minerals in mines.

We note that according to several authors tire wear (which contains about 50% of rubber polymers) is considered as the main contributor of microparticle (MP) emissions into the environment [2].

Rubber wear involves complex physical processes, as has been discussed by Bo Persson [3]. Basically, when a rubber block is sliding on a hard substrate and rubber particles will be removed. The underlying process involves two different steps, namely (a) the nucleation of crack-like defects and (b) the propagation of the cracks, resulting in a detachment of rubber particles, or even small rubber pieces. In the case of fatigue abrasion (mass loss at low severity conditions) while driving on concrete or asphalt road surfaces under low slip-conditions, the size of the detached particles are in the micrometer range (~ 1–$100\ \mu m$). The wear rate is closely related to the frictional processes between the soft rubber and the hard road surface, leading to strong tensile stresses being generated which will drive crack propagation. In the case of high-severity CC wear the average size of detached rubber pieces is much larger. We found that the CC behavior of different tire rubber tread materials correlates with their (stable) crack propagation resistance in relation to high tearing energies below but near their corresponding catastrophic values [4,5].

A reliable direct laboratory prediction of the CC behavior of different rubbers, before the final fabrication of the rubber article (e.g. a tire), is of great importance because of the high costs of product testing in the field. Recently, a rather good correlation was discovered between a rubber

---

* Corresponding author at: Polymer Research Lab s.r.o., Nad Ovčírnou 3685, 76001 Zlín, Czechia.
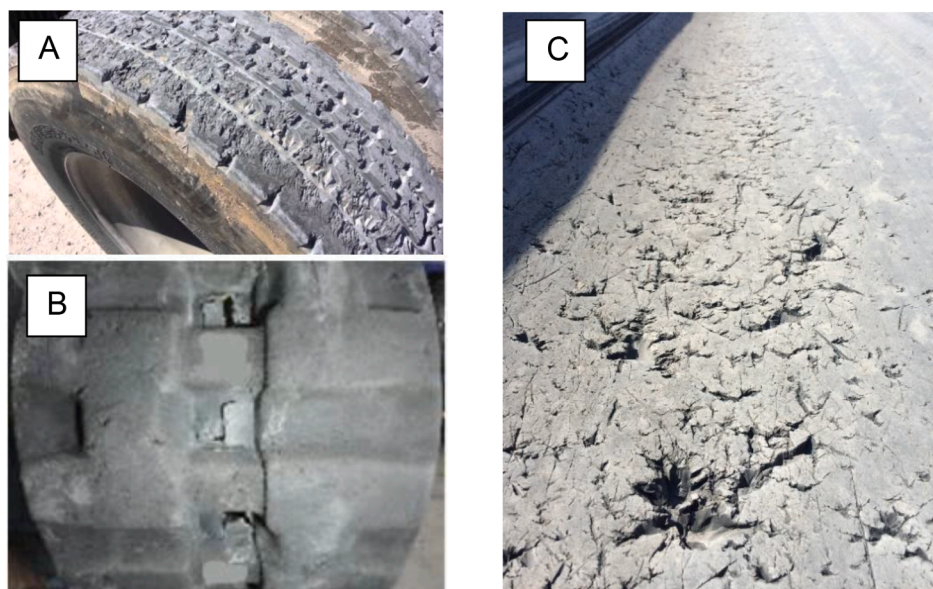 *E-mail address:* radek.stocek@prl-z.com (R. Stoček).

Fig. 1. The Cut & Chip wear phenomena of a truck tire tread (A) [1], a rubber track (B) and a conveyor belt (C).

ranking list of CC laboratory tests with the corresponding ranking list of the tire's CC field protocol [6]. The general principle of lab test methods is based on the assumption that, in the field, pieces of surface material are actually pulled out of the rubber by sharp objects in two steps: "cutting'' and subsequent "chipping''. It was suggested [1,7,8] that cutting occurs when the rubber product strikes a sharp object with sufficient force so that the surface is cut, generating a new surface area. Chipping follows cutting and involves fracturing away of a piece of rubber from the surface. Moreover, the traditional lab CC test methods with small rotating rubber wheels presented e.g. in Refs [1,7-10], employ simple devices, during which loading conditions cannot be applied sufficiently and reproducibly due to the very low applied impact energy, which is not comparable with the real loading conditions of a rubber product, such as a tire. Such simple CC test methods show for certain specimen geometries and loading conditions how the rate of abrasion can be predicted only in a qualitatively approximate manner. Therefore, an advanced testing method and fully instrumented equipment labelled Instrumented Chip and Cut Analyser (ICCA, Coesfeld GmbH, Germany) has been introduced by Stoček et al. [11,12]. The ICCA method is now successfully integrated as a standard lab method in the rubber industry. From the scientific point of view several studies must be still undertaken to describe the influence of various influencing parameters such as the applied normal force, the rotation speed as well as the contact time during an impact. In Refs. [6,12-14] it is shown that the type of rubber polymers and the rubber blend composition significantly influence the CC behavior over the varied range of applied normal forces. It has been shown that in the range of low normal forces (70–130 N), respective low tearing energies, the CC trend of wear resistance for rubber consisting of natural rubber (NR), styrene-butadiene rubber (SBR) or butadiene rubber (BR) is as follow: BR > SBR > NR. However, in the case of a high level of applied normal forces (130–150 N) the

respective tearing energies which one observes opposite wear resistance trends NR > SBR > BR. These observed trends for the different loading regimes correspond with the known fatigue crack growth fracture behavior of the investigated rubber [14,15], in which the low range of tearing energy acts close to abrasion which is usually analyzed using a standard DIN Abrader [12,16] in accordance to ASTM D5963. In this regime BR is the most resistant material in contrast to the regime of high tearing energies in which accelerated crack growth dominates with the most resistant NR material [14-16]. Recently, for the ICCA situation, in the low range of applied normal force at 80 N the local strains have been numerically calculated to be 89% (NR), 83% (SBR) and 74% (BR) [17]. In the case of NR the dedicated strain is still far below the strain values in which strain induced crystallization (SIC) appears. It experimentally has been evaluated that SIC in NR occurs firstly at approximate strain 200% for carbon black (CB) filled and at 400% for unfilled NR [17].

Due to the fact that the previous measurement with ICCA presented results only up to a normal force of 150 N the question arose: How does the CC behavior of the rubbers of interest behave under higher loadings of above 150 N and which role SIC plays in the case of NR under such loading conditions regarding the CC appearance together with the occuring temperature fields?

For this reason the current study is primarily focused on NR, SBR and NR/SBR (50:50) blends. NR is a basic component for highly dynamically loaded rubber products subjected to CC conditions, because it combines a very large elastic strain with a high tensile strength and a remarkable crack growth resistance. These known outstanding properties are obviously attributed to the phenomenon of strain induced crystallization (SIC) [18,19]. On the other side, non-crystallizable SBR is the most consumed synthetic polymer, widely used in place of natural rubber for similar applications, whereas the styrene content lends SBR its wear and abrasion resistance, as well as its strength. Both candidates are very

Table 1
Used rubber compound formulas.

Samples	Composition in phr							
	NR	SBR	CB	ZnO	Stearic acid	6ppd[a]	sulfur	TBBS[b]
NR	100	–	50	2	1	1	2	1
SBR	–	100	50	2	1	1	2	1
NR/SBR	50	50	50	2	1	1	2	1

a) N-(1,3-dimethylbutyl)-N'- phenyl-P-phenylenediamine.
b) N-Tertiarybutyl-2-benzothiazole sulfennamide.

Fig. 2. A photograph of the ICCA (left) and a detailed view into the isolated chamber (right).

promising in terms of the given application and being resistant to CC wear. From the experimental point of view, these materials have been subjected to a broad range of applied normal forces from 90 up to 200 N and the CC characteristics have been studied simultaneously with the temperature development during the CC wear process. We believe that the results will contribute to answering the question: "Why does NR exhibit an excellent resistance against CC wear under high severity conditions and what is the role of SIC during the CC process?"

Experiment and materials

The polymers used in this work are natural rubber (NR, SVR CV6, Vietnam) and non-oil extended cold emulsion copolymerized styrene-butadiene rubber (SBR, Kralex 1500, Synthos Rubbers, Czech republic). Pristine NR as well as SBR and NR/SBR 50/50 blend filled with 50 phr of carbon black CB N330 (Cabot, Czech republic) have been investigated. Table 1 lists the complete formulations of the compounds produced.

A two-step mixing procedure was employed to prepare all rubber compounds. Both of the steps were carried out in an internal mixer SYD-2L (Everplast, Taiwan) with a fill factor of 0.7. First, the masterbatch was prepared after masticating the virgin rubber for 1 min at rotor speed 35 rpm. To this, carbon black was added and then mixed for another 5 min at rotor speed 45 rpm or to reaching the temperature of the mixture

maximum of 150 °C, whereas the initial temperature was 80 °C. The masterbatch thus prepared was milled using a double-roll mill and sheeted out at a rolls temperature of 60 °C. The final batch was then prepared by mixing the masterbatch for 1 min at a rotor speed of 30 rpm and at an initial temperature of 70 °C followed by adding the complete curing system and mixed until the temperature of the mixture reached 105 °C. The final batch was again milled using a double-roll mill at 60 °C of rolls. After storing for 24 h, the curing properties were determined by moving die rheometer MDR 3000 Basic (MonTech, Germany) according to ASTM 6204 at a temperature of 160 °C.

The specimens having different geometries were cured in a heat press LaBEcon 300 (Fontijne Presses, The Netherland) at a temperature of, T_t = 160 °C under the estimated optimum curing time t_{90} + 1 min per 1 mm of the thickness. The cylindrical samples for CC analyses of the geometry 55 mm in diameter and 13 mm in thickness (see e.g. Refs. [12, 13]), standard sheets (150 mm × 150 mm × 2 mm) for the determination of tensile properties as well as plates having 6 mm in thickness used for hardness test were cured.

The tensile properties and Shore-A hardness were measured. The tensile test was performed in accordance to ISO 37 using the universal testing machine (Testometric, UK) at the extension rate of 500 mm/min for standard test specimens of the Type S2 with 2 mm thickness and a distance between the clamps of 35 mm. The tensile properties reported in this paper are averages for 5 specimens. The measurement of the
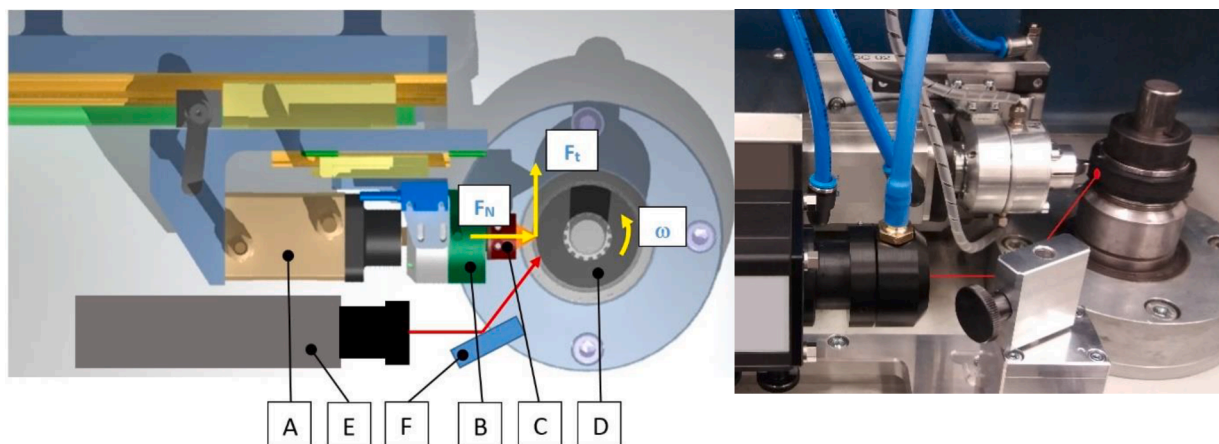

Fig. 3. A schematic of the ICCA measuring principle (left), with: a pneumatic actuator (A); a two-axis load cell (B); a holder + impactor (C); a cylindrical rubber test specimen (D); an IR temperature sensor (E) and a reflective surface for the IR beam direction (F) and a photograph of the ICCA (right) with the location of the spot of temperature measurement.

Table 2
The ICCA testing conditions.

Rotation speed, ω [rev min−1]	Normal force, F_N [N]	Impact frequency, f [Hz]	Time of sliding, t_s [ms]
200	90, 110, 130, 150, 170, 200	5	50

Shore-A hardness was performed in accordance with ISO 7619-1 and measured on 5 samples for each rubber.

Finally, the laboratory CC testing was performed using the Instrumented Chip and Cut Analyser (ICCA, Coesfeld GmbH, Germany), which controls and records applied loads and displacements during a cyclic impact by a rigid indenter to the surface of a solid rubber specimen, whereas 3 replicates have been investigated each applied loading condition. The photograph of the ICCA is shown in Fig. 2.

Fig. 3 (left) shows a detailed scheme of the ICCA inclusive setup for the temperature measurements, whereas Fig. 3 (right) presents the location of the spot of the temperature measurement on the analyzed sample surface. From the scheme the applied counterclockwise rotation of the sample is visible to realize the measurement of the temperature development directly behind the impact. The distance between the location of the impact and the positioned IR beam at the sample surface has been set to be 6 mm (over the perimeter of the sample). In this case the impacted spot arrives under the applied loading condition with a time delay of 10 ms after the impact. Due to measuring the temperature using the reflecting area (see Fig. 3- F) the IR sensor was referenced by the emissivity factor determined at the direct measurement of the sample temperature using a highly-precise contact temperature sensor Fluke 1524-256.

We refer to recent references [11-13,20] regarding the impacting device, the impactor geometry and the description of the independent control of the impact frequency and the sliding time.

As the tangential force is the resulting answer on the impact force, which is assumed to grow proportional with increasing roughness of the penetrated surface, it is taken to calculate the degree of damage in every load cycle. Thus, the key characterization factor evaluated from a multi-channel data acquisition is the CC damage, which is calculated using a numerical algorithm. The tangential force shows an increasing scattering with an increasing time according to an increasing roughness of the sample surface. For this reason an enwrapping curve is calculated which is numerically integrated from a certain starting point $C_{(0)}$ to a cycle count of interest, $C_{(n)}$. Each sum will be divided by the corresponding cycle number $c_{(k)}$ ($0 < k < n$). This (scalar) value quantifies the CC damage at cycle count k and is called "CC damage, P". At least the curve P vs. cycle count (k; $k = 0$ to n) is a description of the CC behavior under the given load conditions. More details on the numerical calculation of the CC damage parameter, P, can be found in previous papers [12,13].

Finally, the CC behaviours of the studied rubbers were evaluated at room temperature using the test conditions listed in Table 2 with simultaneous measurement of the temperature development on the affected sample surface over the complete CC analyses.

Results

The mechanical properties of the rubbers determined from the standard tensile and the Shore A hardness testing are summarized in

Tables 3 and 4. The corresponding physical values of the three rubbers are in a similar magnitude. As expected, the values of the blended material NR/SBR are in between the corresponding values of the pristine NR and SBR rubbers. The stress-strain curves of the rubbers are shown in Fig. 4, in which only one replicate of each rubber is plotted.

The development of the CC damage parameters, P, dependant on the impacting cycles, n, are shown in Fig. 5. First of all, an increasing trend in the CC damage P dependant on the impact cycles is visible, which is caused due to an increase in the number of locally cut and chipped spots from the sample surface with increasing cycle numbers. It is worth mentioning that, P for pristine SBR rubber and NR/SBR blend obviously shows a maximum for the highest applied normal force, $F_N = 200$ N (see Fig. 5, black curves)., However in the case of pristine NR, the maximum P values have been observed at a normal force $F_N = 170$ N ((see Fig. 5, violet curve), whereas applying the normal force $F_N = 200$ N induced a significant decreases of P.

To better understand the CC behavior of the rubbers, we show in Fig. 6 the dependence of P after the final cycle count on the applied normal force, F_N. The dependence of P on F_N for SBR corresponds to the expected trend, in which for low applied normal forces the rubber is marginally subjected to CC damage. However, after reaching a certain critical value (here $F_N = 130$ N) the damage develops steeply with further increasing applied normal forces. For NR, CC damage, P after the final cycle, is more pronounced in the low normal force regime when comparing to the SBR behavior. However, for higher normal forces P approaches a maximum value (here at ∼ 160 N based on data approximation) and decreases with a further increase in F_N, i. e. NR displays a super-resistant behavior against CC damage in a high-severity regime.

Table 4
The Shore A hardness.

Materials	Hardness Shore A
NR	63.3 ± 0.3
SBR	65.0 ± 0.5
NR/SBR	63.4 ± 0.2

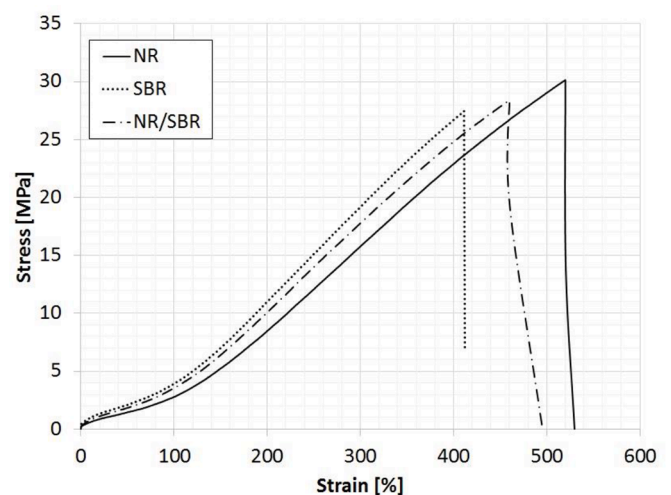**Fig. 4.** The stress–strain curves for all the analysed rubbers.

Table 3
The tensile data.

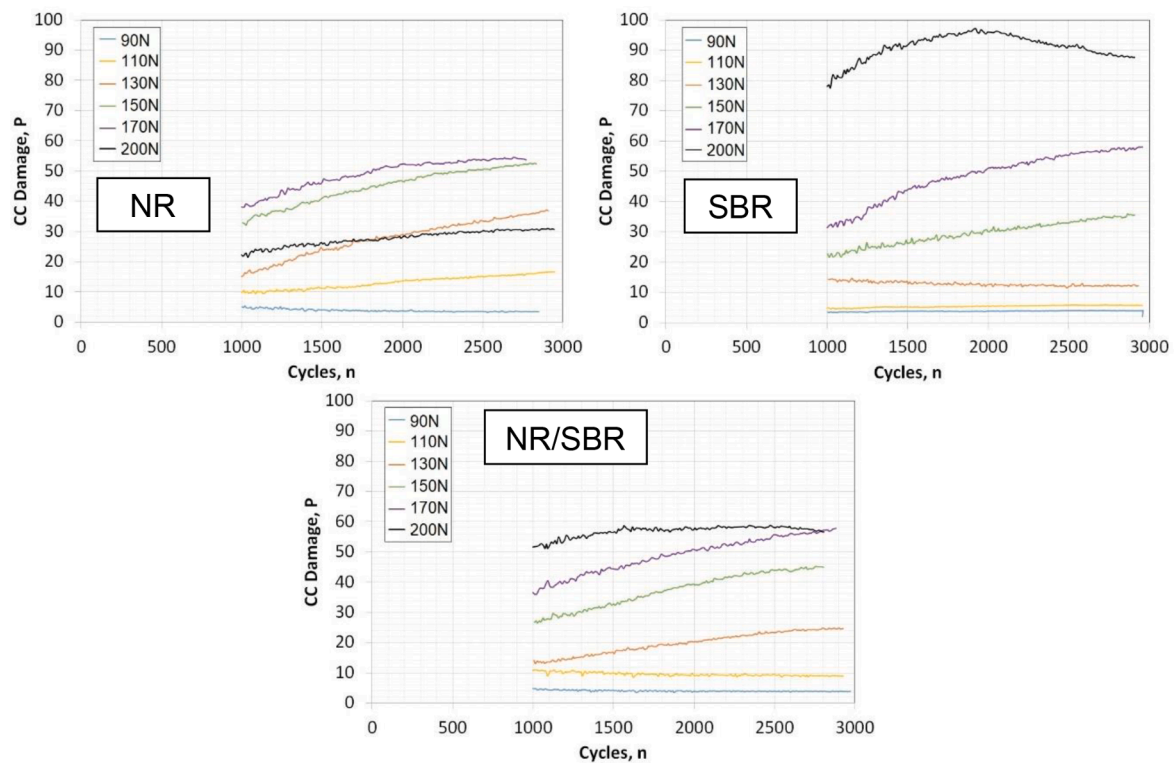| Materials	Stress @ 50% elongation [MPa]	Stress @ 100% elongation [MPa]	Stress @ 300% elongation [MPa]	Stress @ break [MPa]	Strain @ break [%]
NR	1.46±0.07	2.81±0.13	15.51±0.47	28.50±0.58	510.84±11.56
SBR	1.77±0.12	3.34±0.18	16.55±0.38	25.47±0.98	442.43±17.77
NR/SBR	1.67±0.05	3.21±0.11	15.98±0.35	26.11±0.80	479.14±18.22

Fig. 5. *P* versus *n* for all the analysed rubbers. The results are mean values for three test specimens each loading condition.
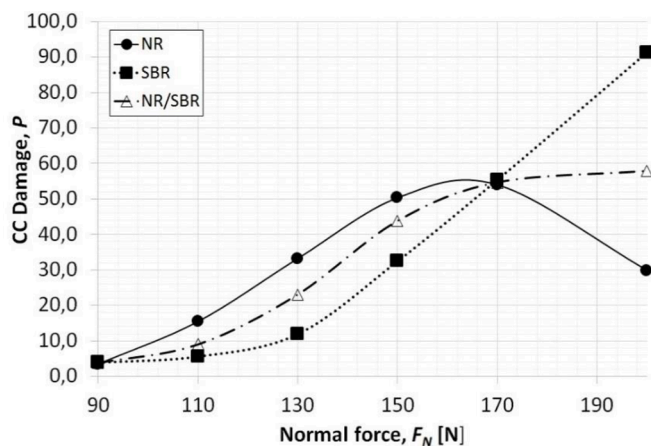

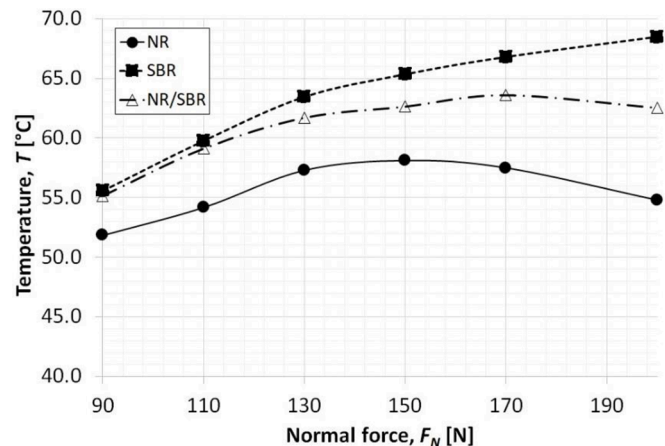**Fig. 6.** *P* versus F_N for all the analysed rubbers at the final cycle count.

Fig. 7. *T* versus F_N for all the analysed rubbers at the final cycle count.

Moreover, it is obvious from Fig. 6 that the CC behavior of the blend NR/SBR lies in between the characteristics of pristine NR and SBR. We assume that the reason for the reversion of the CC damage in NR and the reduction in NR/SBR is an effect of strain-induced crystallization (SIC) of NR when underlying a high strain level [18,19], during which the material becomes stiffer and thus more resistant to crack propagation due to an enhanced resistance of the crystallized rubber chains against rupture and, thus, finally against cut and chip damage. As mentioned in the introduction part, the maximum strain of NR filled with 50 phr of CB during the CC testing process at normal force $F_N = 80$ N has been estimated to be

89% which is below the critical strain value during which SIC appears [17,21]. SIC in NR filled with 50 phr of CB starts to proceed at a strain value of ∼ 200% [21]. Thus, approximating linearly both values 80 N at a strain of 89%, a strain of ∼ 200% during the CC test should appear at a normal force of F_N ∼ 180 N, during which SIC first occurs.

This estimation is in approximate agreement with the experimentally determined and the presented data in Figs. 5 and 6, especially with the onset of CC decline for the NR based rubber and flattened out for the NR/SBR blended rubber (Fig. 6).

Fig. 7 shows the measurements of the temperature, *T*, development over the range of applied normal forces, F_N, as approximation from the last final 100 cycles, whereas the data represent the average values from 3 replicates. The *T* versus F_N curves correspond with the trend of *P* versus F_N presented in Fig. 6. Similar to in Fig. 6, here the temperature development of the NR based materials during a CC process is obviously significantly influenced by the onset of SIC, and this SIC effect is promoted with a higher content of NR. After the onset of the SIC process the temperature decreases significantly at large normal impact forces.

The effect can be qualitatively explained with the help of recent findings about cyclic impact loadings of unfilled and filled natural rubbers using synchrotron wide-angle X-ray scattering (WAXS) coupled

Table 5
Photographs of the ICCA specimens after the final impact cycles for the relevant normal forces for each rubber.

Normal force, F_N [N]	Materials NR	SBR	NR/SBR
90			
110			
130			
150			
170			
200			

with thermography [22], in which dissipative processes during cyclic (tensile) deformations, the heat transfer to the environment, as well as SIC intensity and its time dependence (kinetics) were analyzed. After the loading/unloading impact of a sample spontaneous heating or cooling arises, leading to a thermal equilibration to the environment. The heat exchange is driven by the temperature difference between the surface of the specimen and the environment, depending on the surface area, the heat transmission coefficient and the heat capacity of the sample. Three regions of stress-strain behavior could be distinguished. Below the onset of SIC a certain amount of energy is dissipated within each loading cycle during which the energy loss of a cycle is identical to the heat input into the specimen. The dissipative behavior is responsible for continuously heating the specimen during cyclic loading. After a certain number of cycles, a final equilibrium temperature is reached at which the heat loss to the environment is equal to the dissipated mechanical energy. The equilibrium temperature is normally above the ambient temperature. After the onset of SIC – which is an exothermal process - the heat of the crystallization is responsible for a stronger heating of the sample, and during the subsequent unloading the same amount of energy is released for dissolving the crystallites causing a cooling of the sample. In a region of large deformations, the degree of crystallinity drastically increases (which depends on the amount of filler loading), the rubber partly loses its entropy-elastic character and behaves obviously more as an energy-elastic material without further heating of the sample. More discussions go beyond the scope of this paper. We refer to [19,23-26].

The jagged surfaces of the rubber specimens after the final cycle count of ICCA testing are shown in Table 5. There are the differences between the extent and the features of the damage for the investigated polymers, which are in agreement with previous observations e.g. in Ref. [12]. Looking at Table 5, cracks with distinct angles are visible in the NR based rubber. During the course of the CC damage the cracks grew in length and number which caused them to intersect, and this process led to small chips of rubber being removed from the rubber specimen. When reaching the value of the normal force, $F_N = 130$ N for SBR, the initiated cracks were vertically oriented across the impact path, whereas they appeared to grow deeper into the rubber towards the center of the specimen wheel in contrast to NR. This causes larger chips to be abraded from the surface and thus larger CC damage. While the NR and SBR materials experienced a kind of systematic 'cut and chip' fracture mechanism, the process of crack formation and its evolution for

NR/SBR has obviously a visual character in which the effects of pristine rubbers are mixed.

Conclusion

In this work we reported on the cut and chip (CC) behavior of rubber materials based on NR, SBR and a blend NR/SBR (50/50) over a broad range of applied normal forces (realized with the ICCA) to simulate low up to high severity conditions applied to a rubber product in the field. The mechanical behavior has been investigated and the effect of the strain-induced crystallization (SIC) under high severity conditions has been discussed qualitatively.

We demonstrated that the CC damage for all the analyzed rubbers firstly increases at a low level of normal forces. This increase continues for SBR to high normal force levels. However, for NR the CC damage goes through a maximum, which is obviously caused due to SIC resulting in stiffening the material during cyclic impacts to the rotating wheel. A similar trend has been found for the temperature development versus the normal force.

For the CC damage parameter, P, we obtained the ranking NR > NR/SBR > SBR for low normal forces, whereas the trend is exactly the opposite in the case of high normal forces, i. e. SBR > NR/SBR > NR. Thus, due to the ability of NR to SIC at high loading, respective strains, NR becomes significantly resistant to CC damage under high severity conditions, which mainly appear in typical rubber products applications such as tires, rubber tracks or conveyor belts in the field. We demonstrated how the Instrumented Chip and Cut Analyser (ICCA, produced by Coesfeld GmbH, Germany) is able to predict in a lab similar CC conditions as for rubber products under operating conditions in the field, as described in the introduction.

Declaration of Competing Interest

None.

Funding

References

[1] M. Scherbakov, M.R. Gurvich, A method of wear characterization under cut, chip and chunk conditions, J. Elastom. Plastics 35 (2003) 73–84, https://doi.org/10.1177/009524403031097.

[2] B. Baensch-Baltruschat, B. Kocher, C. Kochleus, F. Stock, G. Reifferscheid, Tyre and road wear particles - a calculation of generation, transport and release to water and soil with special regard to German roads, Sci. Total Environ. 752 (2021), 141939, https://doi.org/10.1016/j.scitotenv.2020.141939.

[3] B.N.J. Persson, Theory of powdery rubber wear, J. Phys.: Condens. Matter 21 (2009), 485001, https://doi.org/10.1088/0953-8984/21/48/485001.

[4] M. Wunde, M. Klüppel, C. Vatterott, J. Tschimmel, J. Lacayo-Pineda, A. Schulze, G. Heinrich, Verbesserung der Laborvorhersagen zum Risswachstum und Verschleiß von LKW-Reifenlaufflächen, Kautschuk Gummi Kunststoffe 72 (2019) 72–78.

[5] R. Stoček, P. Ghosh, A. Machů, J. Chanda, R. Mukhopadhyay, Fatigue crack growth vs. chip and cut wear of NR and NR/SBR blend-based rubber compounds, in: G. Heinrich, R. Kipscholl, R. Stoček (Eds.), Fatigue Crack Growth in Rubber Materials. Advances in Polymer Science, Vol 286, Springer, Cham, 2020, https://doi.org/10.1007/12_2020_67.

[6] R. Stoček, G. Heinrich, A. Schulze, M. Wunde, M. Klüppel, C. Vatterott, J. Tschimmel, J. Lacayo-Pineda, R. Kipscholl, Chip & Cut Wear of Truck Tire Treads: comparison between laboratory and real Tire Testing, Kautschuk Gummi Kunststoffe 73 (2020) 51–55, 6.

[7] Beatty, J.R. (1979). Testing Apparatus and Method for Measuring Cutting, Chipping and Abrasion Resistance, U.S. Patent 4,144,740.

[8] J. Beatty, B. Miksch, A laboratory cutting and chipping tester for evaluation off-the-road and heavy-duty tire treads, Rubber Chem. Technol. 55 (1982) 1531–1546, https://doi.org/10.5254/1.3535947, doi.org/.

[9] C. Nah, B.W. Jo, S. Kaang, Cut and chip resistance of NR–BR blend compounds, J. Appl. Polym. Sci. 68 (1998) 1537–1541, https://doi.org/10.1002/(SICI)1097-4628(19980531)68:9<1537::AID-APP17>3.0.CO;2-W.

[10] J.-.H. Ma, Y.-.X. Wang, L.-.Q. Zhang, Y.-.P. Wu, Improvement of cutting and chipping resistance of carbon black-filled styrene butadiene rubber by addition of nanodispersed clay, J. Appl. Polym. Sci. 125 (2012) 3484–3489, https://doi.org/10.1002/app.36710.

[11] R. Stoček, W.V. Mars, C.G. Robertson, R. Kipscholl, Characterizing rubber's resistance against chip and cut behaviour, Rubber world 257 (2018) 38–40.

[12] R. Stoček, W.V. Mars, R. Kipscholl, C.G. Robertson, Characterisation of cut and chip behaviour for NR, SBR and BR compounds with an instrumented laboratory device, Plastics, Rubber Comp. 48 (2019) 14–23, https://doi.org/10.1080/14658011.2018.1468161.

[13] R. Kipscholl, R. Stoček, Quantification of chip and cut behaviour of basic rubber (NR, SBR), RFP Rubber Fibres Plastics 02 (2019) 88–91.

[14] G.J. Lake, P.B. Lindley, The mechanical fatigue limit for rubber, J. Appl. Polym. Sci. 9 (1965) 1233–1251, https://doi.org/10.1002/app.1965.070090405.

[15] R. Stoček, M. Stěnička, P. Zádrapa, Future trends in predicting the complex fracture behaviour of rubber materials, Continuum Mech. Thermodyn. 33 (2021) 291–305, https://doi.org/10.1007/s00161-020-00887-z.

[16] C.G. Robertson, W.V. Mars, R. Stoček, R. Kipscholl, Characterizing durability of rubber for tires, Tire Technol. Int. (2019) 78–82.

[17] C.G. Robertston, J.D. Suter, M.A. Bauman, R. Stoček, W.V. Mars, Finite element modeling and critical plane analysis of a cut-and-chip experiment for rubber, Tire Sci. Technol., TSTCA 48 (2020), https://doi.org/10.2346/tire.20.190221.

[18] K. Brüning, K. Schneider, S.V. Roth, G. Heinrich, Strain-induced crystallization around a crack tip in natural rubber under dynamic load more, Polymer (Guildf) 54 (2013) 6200–6205, https://doi.org/10.1016/j.polymer.2013.08.045.

[19] K. Brüning, K. Schneider, S. Roth, G. Heinrich, Kinetics of strain-induced crystallization in natural rubber: a diffusion-controlled rate law, Polymer (Guildf) 72 (2015) 52–58, https://doi.org/10.1021/ma3011476.

[20] E. Euchler, H. Michael, M. Gehde, O. Kratina, R. Stoček, Wear of technical rubber materials under cyclic impact loading conditions, Kautschuk Gummi Kunststoffe 69 (2016) 22–26.

[21] S. Trabelsi, P.-.A. Albouy, J. Rault, Effective local deformation in stretched filled rubber, Macromolecules 36 (2003) 9093–9099, https://doi.org/10.1021/ma0303566.

[22] K. Schneider, L. Zybell, J. Domurath, G. Heinrich, S.V. Roth, A. Rothkirch, W. Ohm, Investigation of time dependence of dissipation and strain induced crystallization in natural rubber under cyclic and impact loading, in: A. Lion, M. Johlitz (Eds.), Constitutive Models for Rubber X: Proceedings of the European Conference on Constitutive Models for Rubbers X (Munich, Germany, 28-31 August 2017), CRC Press/Balkema, 2017, pp. 173–177.

[23] K. Brüning, K. Schneider, G. Heinrich, Situ Structural Characterization of Rubber during Deformation and Fracture, in: W. Grellmann, G. Heinrich, M. Kaliske, M. Klüppel, K. Schneider, T. Vilgis (Eds.), Fracture Mechanics and Statistical Mechanics of Reinforced Elastomeric Blends. Lecture Notes in Applied and Computational Mechanics, Vol 70, Springer, Berlin, Heidelberg, 2013, https://doi.org/10.1007/978-3-642-37910-9_2.

[24] K. Brüning, K. Schneider, S.V. Roth, G. Heinrich, Kinetics of Strain-Induced Crystallization in Natural Rubber Studied by WAXD: dynamic and Impact Tensile Experiments, Macromolecules 45 (2012) 7914–7919, https://doi.org/10.1021/ma3011476, 19.

[25] J.B. LeCam, J.R. Samanca Martinez, X. Balandraud, E. Toussaint, J. Caillard, Revisiting the mechanisms involved in rubber deformation using experimental thermomechanics, in: B. Marvalová, I. Petríková (Eds.), Constitutive models for rubbers IX: 3-11, CRC Press, 2015. Boca Raton et al.:.

[26] T. Spratte, J. Plagge, M. Wunde, M. Klüppel, Investigation of strain-induced crystallization of carbon black and silica filled natural rubber composites based on mechanical and temperature measurements, Polymer (Guildf) 115 (2017) 12–20, https://doi.org/10.1016/j.polymer.2017.03.019.